Journal of Power Sources 186 (2009) 334–338

Contents lists available at ScienceDirect

Journal of Power Sources

journal homepage: www.elsevier.com/locate/jpowsour

Short communication

Chemical degradation of proton conducting perflurosulfonic acid ionomer membranes studied by solid-state nuclear magnetic resonance spectroscopy

L. Ghassemzadeh[a,b], M. Marrony[c], R. Barrera[d], K.D. Kreuer[a], J. Maier[a], K. Müller[b,*]

[a] Max-Planck-Institut für Festkörperforschung, Heisenbergstraße 1, D-70569 Stuttgart, Germany
[b] Institut für Physikalische Chemie, Universität Stuttgart, Pfaffenwaldring 55, D-70569 Stuttgart, Germany
[c] European Institute for Energy Research, Emmy-Noether-Strasse 11, D-76131 Karlsruhe, Germany
[d] Edison, Via Giorgio La Pira, 2, I-10028 Trofarello, Italy

ARTICLE INFO

Article history:
Received 18 July 2008
Received in revised form 1 October 2008
Accepted 5 October 2008
Available online 11 October 2008

Keywords:
Fuel cell
In situ degradation test
Nafion
Hyflon Ion
Solid-state NMR

ABSTRACT

The degradation of two different types of perfluorinated polymer membranes, Nafion and Hyflon Ion, has been examined by solid-state ^{19}F and ^{13}C NMR spectroscopy. This spectroscopic technique is demonstrated to be a valuable tool for the study of the membrane structure and its alterations after in situ degradation in a fuel cell. The structural changes in different parts of the polymers are clearly distinguished, which provides unique insight into details of the degradation processes. The experimental NMR spectra prove that degradation mostly takes place within the polymer side chains, as reflected by the intensity losses of NMR signals associated with SO_3H, CF_3, OCF_2 and CF groups. The integral degree of degradation is found to decrease with increasing membrane thickness while for a given thickness, Hyflon Ion appears to degrade less than Nafion.

1. Introduction

Membrane degradation in fuel cell results from a combination of different phenomena including mechanical, thermal, chemical and electrochemical aging. Low relative humidity [1–4] and temperatures above 90 °C [1–3,5] as well as the presence of ionic contaminants [2,6–13] can accelerate membrane degradation.

For fuel cell membranes, oxidation–reduction reactions and acid–base hydrolytic reactions are equally possible. The membrane is in direct contact with an oxidizing environment on the cathodic and chemically reducing environment on the anodic side, and it is subjected to various water activities. In the literature, different mechanisms for chemical degradation are discussed which involve the cross-over of H_2 or O_2 [2,14–18], oxygen reduction at the cathode [19] and radical attacks [7–10,15,20–23]. Diffusion of H_2O_2 into the membrane and reaction with metallic impurities can be the source for hydroxy and peroxy radical formation [4,8,9,24–26]. The progressive attack of main chain endgroups by these radicals is considered an important degradation pathway of proton conducting polymer membranes [27,28]. Such reactions have been suggested to start from reactive endgroups such as COOH which are formed during the polymer manufacturing process and may be present in the polymer in small quantities [27,29,30].

So far, most degradation studies rely on the chemical analysis of fuel cell effluents or the solution after ex situ Fenton's test. A standard parameter to quantify degradation levels is the amount of released F^- ions [11,14,15,17,18,31]. Apart from spectroscopic techniques such as broadband dielectric spectroscopy [32], EPR [7,8,10,22,23,33–35], FTIR [6,9,24,25,30] and XPS [6,36], in particular mass spectroscopy and liquid-state NMR [37] have been used to identify degradation products other than fluoride ions generated during fuel cell operation.

In the present work the chemical changes of the membrane itself (Nafion [38] and Hyflon Ion [20,39]) is studied directly by solid-state NMR spectroscopy, where ^{13}C CP/MAS [40] and ^{19}F NMR spectra are recorded before and after in situ fuel cell tests. It is shown that degradation depends on membrane thickness and polymer architecture, and the most reactive molecular segments are identified.

2. Experimental

2.1. Materials

Two types of perfluorosulfonic acid membranes, Nafion of different thickness (Nafion 112, 115 and 117) and Hyflon Ion type E87, which differ in the lengths of their side chains and their

* Corresponding author. Tel.: +49 711 6856 4470; fax: +49 711 6856 4467.
E-mail address: k.mueller@ipc.uni-stuttgart.de (K. Müller).

0378-7753/$ – see front matter © 2008 Elsevier B.V. All rights reserved.
doi:10.1016/j.jpowsour.2008.10.004

Nafion:

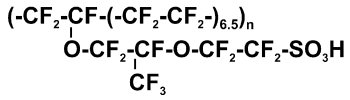

Hyflon Ion:

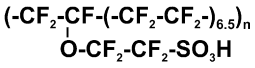

Fig. 1. Chemical structures of Nafion and Hyflon Ion.

Table 1
Properties of the perfluorinated membranes investigated in this work.

Membrane	Supplier	Thickness (in.) wet	Ion-exchange capacity (meqiv. g^{-1} dry SPE)
Nafion 112	Hydro2Power SRL	0.002	0.9
Nafion 115	Hydro2Power SRL	0.005	0.9
Nafion 117	Hydro2Power SRL	0.007	0.9
Hyflon Ion E87	Solvay Solexis S.p.A.	0.00078	1.15

ion-exchange capacity (see Fig. 1), were used in this study. Nafion samples were obtained from Hydro2Power SRL (Milan, Italy) and Hyflon Ion membrane from Solvay Solexis S.p.A. (Bollate, Italy). The relevant material parameters are summarized in Table 1.

2.2. Membrane pre-conditioning

Membranes (size: 5.5 cm^2) were soaked in 250 ml H_2O_2 (3 vol%) at 60 °C for 1 h to remove any organic impurities. After rinsing with deionized water, the membranes were soaked in 250 ml H_2SO_4 (1 M) at 60 °C for 1 h to remove all metallic impurities and to exchange all cations for H^+. Finally, the membranes were boiled in deionized water at 100 °C for 1 h.

2.3. Fuel cell tests

E-TEK LT250EW electrodes (0.5 mg Pt/cm^2 and 0.7 mg Nafion/cm^2) were used for the membrane-electrodes assembly (MEA) during the fuel cell tests. A torque of 3 nm is applied at ambient temperature for the cell assembly, having 5 cm^2 of active surface area, to allow reasonable electrode-membrane contacts. The gas pressures were kept at $p = 1.5$ bar with flows corresponding to a stoichiometry of 1.5/2 for H_2 and O_2.

At the beginning of each test the cells were activated by inlet gases of 100% relative humidity. The cell was then heated to 70 °C with a temperature ramp of 5 °C per hour, and a potential of $E = 0.65$–0.7 V was applied to the cell by adjusting the current. A by-pass system also allowed for dry-gases mode. Some cycling electrical loading steps were then performed simulating the hydration and dehydration behavior of the membrane likely to be encountered during long term operation. The experimental procedure provided one open circuit voltage event (OCV) per hour which lasted 30 s, after which the system returned to the initial value for the current density.

In the same way, long time tests at operating temperatures of 80–90 °C were performed by adjusting the current in order to maintain a potential of 0.65–0.7 V. The end of the test was reached after 150 loading cycles or after mechanical rupture of the membrane as indicated by a sudden potential drop. Details of the test protocols are reported elsewhere [41].

Following the fuel cell tests and after carefully removing the electrodes and the gas diffusion layer, the membranes were dried in a vacuum oven at 110 °C for 24 h and packed into the NMR rotors.

2.4. NMR spectroscopy

All NMR experiments were performed at 100.53 MHz for ^{13}C and 376.09 MHz for ^{19}F on a Varian InfinityPlus 400 NMR spectrometer. The NMR spectra were acquired under MAS conditions using a 4-mm HFXY magic-angle spinning probe at a spinning frequency of 15 kHz. ^{19}F NMR spectra were recorded with a recycle delay of 2 s and a dwell time of 5 μs. Here, the ^{19}F 90° pulse length was 3 μs. $^{13}C\{^{19}F\}$ CP/MAS NMR spectra were taken by means of the RAMP-CP sequence and xy-16 pulse decoupling [40], a contact time of 1.6 ms and a recycle delay of 2 s (^{13}C 90° pulse width: 2.8 μs, ^{19}F decoupling power 89 kHz). Teflon was utilized for establishing the Hartmann–Hahn match. The ^{19}F NMR signal of Teflon at −121 ppm (relative to $CFCl_3$ with $\delta = 0$ ppm) and the ^{13}C NMR signal of adamantane at 38.56 ppm (relative to TMS with $\delta = 0$ ppm) were used as secondary external references. All experiments were performed at 80 °C which provided a better spectral resolution.

3. Results and discussion

Nafion membranes of different thicknesses and a Hyflon Ion membrane were investigated in the present work. These polymers consist of a perfluorinated polymer backbone and ether-linked perfluorinated side chains of different lengths with a sulfonic end-group. The shorter side chains of the Hyflon Ion structure results, compared to Nafion, in a higher concentration of SO_3H groups for the same degree of branching (Fig. 1). The short side chain membranes have a higher degree of crystallinity and higher glass transition temperature (T_g) as compared to the Nafion membrane with the longer side chains [20,39].

These properties have been suggested to be the reason for less swelling, higher conductivity, lower electroosmotic drag [42] and better mechanical stability especially at high temperature and, as a consequence, better performance in the temperature range between 80 and 120 °C [20,39,42]. The relevant material parameters are summarized in Table 1.

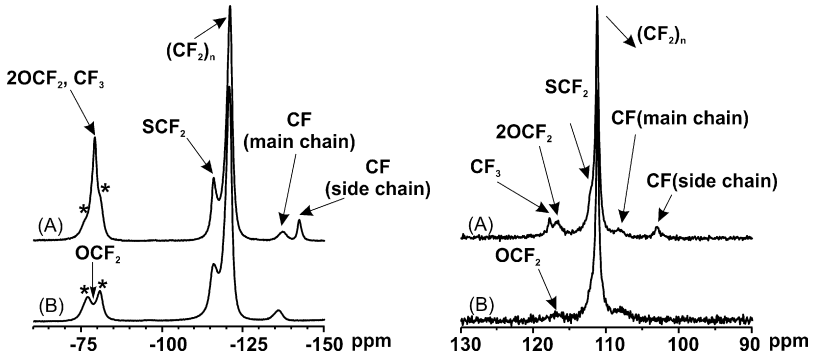

Fig. 2. ^{19}F NMR (left) and $^{13}C\{^{19}F\}$ CP/MAS NMR spectra (right) of Nafion (A) and Hyflon Ion (B). Asterisks indicate spinning sidebands.

Table 2
Chemical shift values (in ppm) and assignment of the ^{13}C and ^{19}F resonances in Nafion and Hyflon Ion membranes[a].

	CF (side chain)	CF (main chain)	$(CF_2)_n$	SCF_2	OCF_2	CF_3
^{19}F						
Nafion	−144	−138	−121	−117	−80.1 79.9	−80
Hyflon Ion	–	−138	−121	−117	−80	–
^{13}C						
Nafion	103.4	108.2	111.4	113	116.7 117	118
Hyflon Ion	–	108.2	111.4	113	117	–

[a] From signal deconvolution and following Ref. [41].

^{19}F and $^{13}C\{^{19}F\}$ CP/MAS spectra for Nafion 117 and Hyflon Ion prior to the in situ test are shown in Fig. 2. The ^{13}C and ^{19}F resonances of Nafion were assigned on the basis of a former investigation by Chen and Schmidt-Rohr [43], and are listed in Table 2.

The NMR spectra were measured at an elevated temperature of 80 °C, which – as demonstrated by the spectra given in Fig. 2 – provided a satisfactory resolution. It should be mentioned that the ^{19}F NMR spectrum of a completely dry membrane, recorded at room temperature, is much less resolved. For instance, the signal associated with the SCF_2 segment only appears as a lowfield shoulder next to the dominant CF_2 signal. In principle, a better resolution could also be achieved by higher sample spinning rates which unfortunately were not available in the present study. However, it has been shown that even a spinning rate of 30 kHz was not sufficient to resolve these signals [43].

The backbones of the present fluoropolymers are identical and consist of CF_2 and CF groups. The CF_2 groups give rise to resonances at −121 and 111.4 ppm in the ^{19}F and ^{13}C NMR spectra, respectively. Likewise, the ^{19}F resonance at −138 ppm and the ^{13}C signal at 108.2 ppm are signatures of the backbone CF groups.

The common $–O–CF_2–CF_2–SO_3H$ unit is clearly identified in the ^{13}C and ^{19}F NMR spectra of the Nafion and Hyflon Ion membranes. The ^{19}F resonance at −117 ppm and the shoulder at 113 ppm in the ^{13}C NMR spectrum reflect the SCF_2 groups, while the OCF_2 group of this common structural unit gives rise to a signal at −80 ppm in the ^{19}F NMR spectra. For Nafion the OCF_2 group appears in a broad peak which is dominated by the CF_3 resonance at −80 ppm and the spinning sidebands from the CF_2 and SCF_2 signals. In the spectrum of Hyflon Ion the spinning sidebands are clearly separated while the

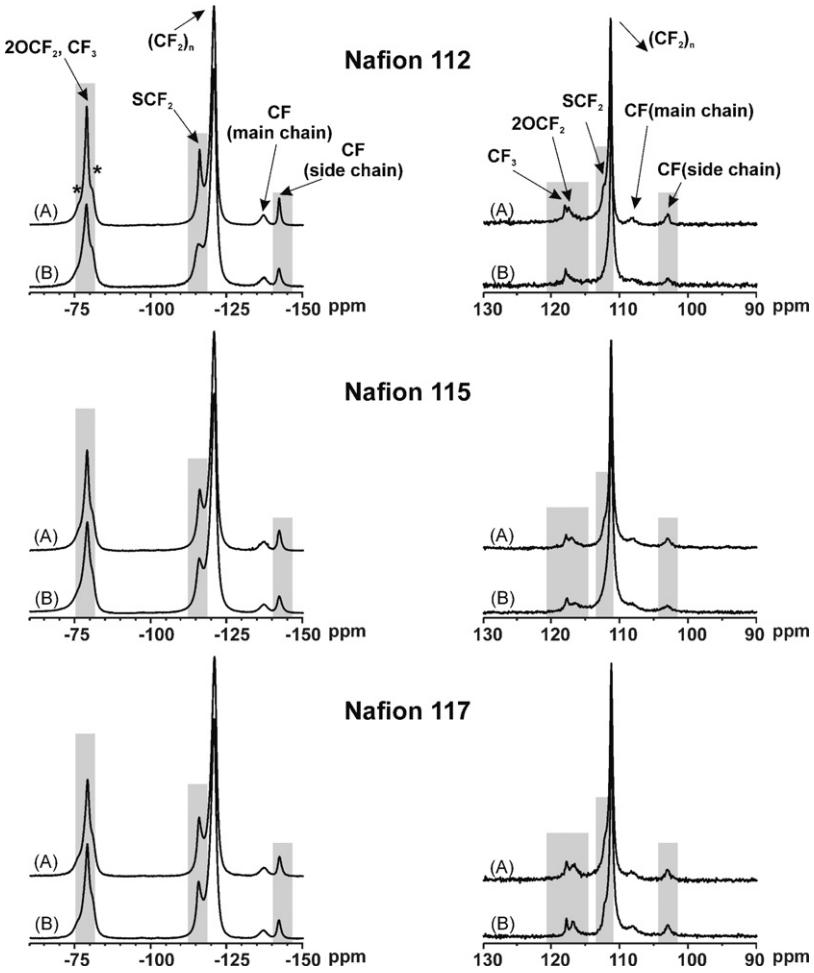

Fig. 3. ^{19}F NMR (left) and $^{13}C\{^{19}F\}$ CP/MAS NMR spectra (right) of Nafion membranes of different thicknesses, before (A) and after (B) in situ tests. Asterisks indicate spinning sidebands.

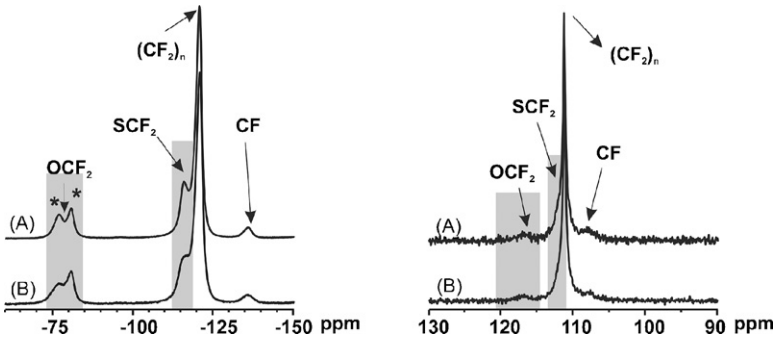

Fig. 4. ^{19}F NMR (left) and $^{13}C\{^{19}F\}$ CP/MAS NMR spectra (right) of Hyflon Ion before (A) and after (B) the in situ tests. Asterisks indicate spinning sidebands.

signals from the CF_3 group are missing. In the ^{13}C NMR spectrum the OCF_2 group appears as a broad resonance at 117 ppm.

The Nafion and Hyflon Ion membranes differ in the lengths of the side chains, and the side chain of Hyflon Ion does not contain the –O–CF_2–$CF(CF_3)$– segment next to the polymer backbone (see Fig. 1). These structural differences are directly visible in the ^{19}F and ^{13}C NMR spectra: for Nafion additional ^{19}F and ^{13}C resonances at −144 and 103.4 ppm, respectively, stemming from side chain CF_2 units appear. The CF_3 group causes a sharp ^{13}C signal at 118 ppm, while in the ^{19}F NMR spectrum, the ^{19}F resonance of this structural unit coincides with the OCF_2 group and signals from spinning sidebands, as mentioned above.

Typical ^{19}F and ^{13}C NMR spectra for Nafion and Hyflon Ion samples before and after degradation are shown in Figs. 3 and 4. The spectra are normalized to the dominant peak of the backbone CF_2 groups. It is found that after the fuel cell tests the intensities of the side chain signals (arising from SCF_2, CF_3, OCF_2 and CF groups) have decreased in all polymer samples. The present solid-state NMR data therefore support the assumption that the pendant side chains of the ionomers are more affected than the main chain [10,23,37]. In general, the changes after in situ tests are better traceable in the ^{19}F than in the ^{13}C NMR spectra which is related to the higher sensitivity and the better resolution of the former ones.

A better comparison of the structural changes due to membrane degradation after fuel cell in situ tests is possible by inspection of the plots given in Fig. 5. They show the ratios of the peak intensities after and before the fuel cell tests for all investigated polymer membranes. As noted above, the spectra were normalized to the peak of the main chain $(CF_2)_n$ units, and possible changes due to main chain degradation are therefore not detectable.

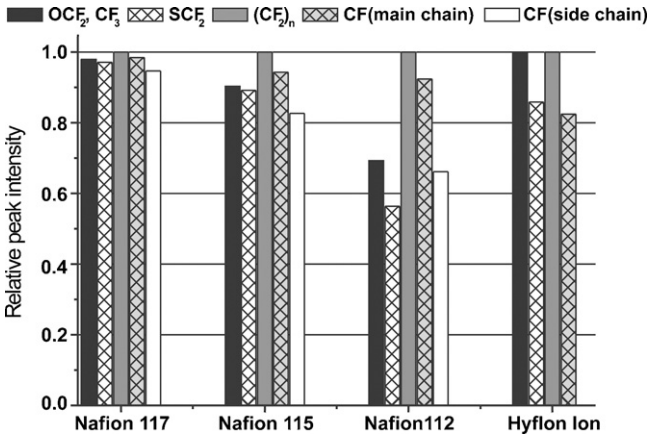

Fig. 5. Relative peak heights of the various structural units after the in situ tests. The given numbers are the ratios of the peak intensities after the in situ tests relative to the original intensities before the tests in percentage, as taken from the ^{19}F NMR spectra. For Hyflon Ion, the black column refers only to the OCF_2 group (see text).

From these plots, the following conclusions are drawn:

- Degradation of the side groups is verified for all membranes.
- For Nafion, degradation increases with decreasing membrane thickness (in the order Nafion 117, Nafion 115 and Nafion 112).
- Although the Hyflon Ion sample is the thinnest of all membranes, it is almost as stable as Nafion 115 and Nafion 117.

At this point, there is no unambiguous explanation for the observed trends, because relevant data are still missing. In general, the rate of formation of aggressive radicals and the reactivity of the ionomer itself have to be considered. A trivial explanation could be a degradation process proceeding from the membrane surface, which is expected to affect thin membranes more than thicker membranes. But the thickness dependence of the degradation may also be the result of a decreasing gas cross-over with thickness, if peroxo radical (e.g. $HO_2^{\bullet}$) formation were rate limiting the degradation process, and if the formation of such radicals on the catalyst surface were controlled by either H_2 cross-over to the cathode side or O_2 cross-over to the anode side [44]. The latter explanation may also provide a rational for understanding the higher durability of the Hyflon Ion membrane. Because of their higher crystallinity, short side chain ionomers such as Hyflon Ion usually swell less [42], which is anticipated to also reduce gas cross-over especially at elevated operation temperature [44].

Another possible explanation for the relative stability of Hyflon Ion is its lower concentration of chemically sensitive ether linkages. Reaction with the only ether group close to the polymer backbone may even be hindered sterically.

In order to discriminate between these explanations, the degradation conditions may be varied and the anode and cathode side of the membrane may be analysed separately. Work along these lines is in progress and will be published elsewhere.

There are so far only two reports on the application of solid-state ^{19}F NMR spectroscopy for the study of Nafion degradation [9,24]. In both cases, the Fenton reaction has been used for preparing samples via ex situ treatment. It is known that the ex situ Fenton reaction generally gives rise to stronger degradation than in situ tests. Surprisingly, both of these former NMR investigations revealed only slight differences between the structural composition of the ionomer membranes before and after ex situ degradation. Moreover, the structural changes derived from these former ex situ studies were even less than those found in the present solid-state NMR investigations dealing with in situ degradation. At present, we cannot explain these discrepancies.

However, it should be noted that in recent solid-state NMR and IR studies of samples from ex situ tests, performed in our group, again pronounced structural changes for such ionomer membranes have been registered [45]. It was found that the presence of a high concentration of iron ions, which are paramagnetic, is accompanied by severe changes of the NMR signal intensities, and the derived

NMR and IR data at first sight appeared to be inconsistent. For a quantitative discussion of such solid-state NMR investigations it is thus absolutely necessary that any effects on the signal intensities due to interaction with paramagnetic species can be ruled out. Further investigations, addressing the role of paramagnetic impurities (e.g. Fe^{3+}) in the degradation process and for the NMR analysis are under way [45].

4. Conclusions

Solid-state NMR spectroscopy has been successfully introduced as a new method for the study of the structural changes within perfluorosulfonic acid membranes after fuel cell in situ tests. Unlike most other techniques, the present method provides the opportunity to directly study the structural alterations of the membranes. The results of ^{19}F and ^{13}C NMR measurements before and after in situ tests demonstrate that degradation predominantly takes place in the side chains containing SO_3H, CF_3, OCF_2 and CF groups. Degradation is decreasing with increasing membrane thickness and, for a given thickness, degradation for short side chain Hyflon Ion membranes is found to be less severe.

However, much more work is necessary to get a comprehensive understanding of the degradation mechanisms in such membrane systems. Therefore, further studies involving the present spectroscopic techniques for direct study of polymer degradation are in progress.

Acknowledgments

The authors thank Dr. Matthias Gebert (Solvay Solexis S.p.A.) for providing Hyflon Ion type membranes. L. Ghassemzadeh would like to thank for the financial support by the International Max-Planck Research School for Advanced Materials.

M. Marrony and R. Barrera gratefully acknowledge financial support by the European Commission under the FP6 program (IP AUTOBRANE).

References

[1] V.A. Sethuraman, J.W. Weidner, A.T. Haug, L.V. Protsailo, Journal of the Electrochemical Society 155 (2008) B119–B124.
[2] M. Inaba, T. Kinumoto, M. Kiriake, R. Umebayashi, A. Tasaka, Z. Ogumi, Electrochimica Acta 51 (2006) 5746–5753.
[3] S.D. Knights, Journal of Power Sources 127 (2004) 127–134.
[4] E. Endoh, Electrochemical and Solid State Letters 7 (2004) A209–A211.
[5] Y. Shibahara, Y. Akiyama, Y. Izumi, S. Nishijima, Y. Honda, N. Kimura, S. Tagawa, G. Isoyama, Journal of Polymer Science Part B: Polymer Physics 46 (2008) 1–7.
[6] C. Chen, G. Levitin, D.W. Hess, T.F. Fuller, Journal of Power Sources 169 (2007) 288–295.
[7] A. Bosnjakovic, M.K. Kadirov, S. Schlick, Research on Chemical Intermediates 33 (2007) 677–687.
[8] M. Danilczuk, A. Bosnjakovic, M.K. Kadirov, S. Schlick, Journal of Power Sources 172 (2007) 78–82.
[9] T. Kinumoto, M. Inaba, Y. Nakayama, K. Ogata, R. Umebayashi, A. Tasaka, Y. Iriyama, T. Abe, Z. Ogumi, Journal of Power Sources 158 (2006) 1222–1228.
[10] A. Bosnjakovic, S. Schlick, Journal of Physical Chemistry B 108 (2004) 4332–4337.
[11] A. Pozio, R.F. Silva, M. De Francesco, L. Giorgi, Electrochimica Acta 48 (2003) 1543–1549.
[12] T. Okada, Y. Ayato, H. Satou, M. Yuasa, I. Sekine, Journal of Physical Chemistry B 105 (2001) 6980–6986.
[13] R. Bauer, G. Waldner, H. Fallmann, S. Hager, M. Klare, T. Krutzler, S. Malato, P. Maletzky, Catalysis Today 53 (1999) 131–144.
[14] V.O. Mittal, H.R. Kunz, J.M. Fenton, Journal of the Electrochemical Society 154 (2007) B652–B656.
[15] M. Aoki, H. Uchida, M. Watanabe, Electrochemistry Communications 8 (2006) 1509–1513.
[16] J.R. Yu, T. Matsuura, Y. Yoshikawa, M.N. Islam, M. Hori, Electrochemical and Solid State Letters 8 (2005) A156–A158.
[17] M. Aoki, H. Uchida, M. Watanabe, Electrochemistry Communications 7 (2005) 1434–1438.
[18] V.O. Mittal, H.R. Kunz, J.M. Fenton, Journal of the Electrochemical Society 153 (2006) A1755–A1759.
[19] J.R. Yu, B.L. Yi, D.M. Xing, F.Q. Liu, Z.G. Shao, Y.Z. Fu, Physical Chemistry Chemical Physics 5 (2003) 611–615.
[20] L. Merlo, A. Ghielmi, L. Cirillo, M. Gebert, V. Arcella, Journal of Power Sources 171 (2007) 140–147.
[21] A. Panchenko, Journal of Membrane Science 278 (2006) 269–278.
[22] S. Mitov, B. Vogel, E. Roduner, H. Zhang, X. Zhu, V. Gogel, L. Jorissen, M. Hein, D. Xing, F. Schonberger, J. Kerres, Fuel Cells 6 (2006) 413–424.
[23] M.K. Kadirov, A. Bosnjakovic, S. Schlick, Journal of Physical Chemistry B 109 (2005) 7664–7670.
[24] H.L. Tang, P.K. Shen, S.P. Jiang, W. Fang, P. Mu, Journal of Power Sources 170 (2007) 85–92.
[25] J.L. Qiao, M. Saito, K. Hayamizu, T. Okada, Journal of the Electrochemical Society 153 (2006) A967–A974.
[26] G. Hubner, E. Roduner, Journal of Materials Chemistry 9 (1999) 409–418.
[27] D.E. Curtin, R.D. Lousenberg, T.J. Henry, P.C. Tangeman, M.E. Tisack, Journal of Power Sources 131 (2004) 41–48.
[28] A. LaConti, M. Hamdan, R. McDonald, Handbook of Fuel Cells: Fundamentals, Technology, and Applications, 2003, pp. 647–662.
[29] C. Zhou, M.A. Guerra, Z.M. Qiu, T.A. Zawodzinski, D.A. Schiraldi, Macromolecules 40 (2007) 8695–8707.
[30] T. Xie, C.A. Hayden, Polymer 48 (2007) 5497–5506.
[31] W. Liu, K. Ruth, G. Rusch, Journal of New Materials for Electrochemical Systems 4 (2001) 227–232.
[32] D.W. Rhoades, M.K. Hassan, S.J. Osborn, R.B. Moore, K.A. Mauritz, Journal of Power Sources 172 (2007) 72–77.
[33] A. Panchenko, H. Dilger, E. Moller, T. Sixt, E. Roduner, Journal of Power Sources 127 (2004) 325–330.
[34] A. Lund, L.D. Macomber, M. Danilczuk, J.E. Stevens, S. Schlick, Journal of Physical Chemistry B 111 (2007) 9484–9491.
[35] A. Panchenko, H. Dilger, J. Kerres, M. Hein, A. Ullrich, T. Kaz, E. Roduner, Physical Chemistry Chemical Physics 6 (2004) 2891–2894.
[36] C.D. Huang, K.S. Tan, H.Y. Lin, K.L. Tan, Chemical Physics Letters 371 (2003) 80–85.
[37] J. Healy, C. Hayden, T. Xie, K. Olson, R. Waldo, A. Brundage, H. Gasteiger, J. Abbott, Fuel Cells 5 (2005) 302–308.
[38] K.A. Mauritz, R.B. Moore, Chemical Reviews 104 (2004) 4535–4585.
[39] L. Merlo, A. Ghielmi, L. Cirillo, M. Gebert, V. Arcella, Separation Science and Technology 42 (2007) 2891–2908.
[40] S.F. Liu, K. Schmidt-Rohr, Macromolecules 34 (2001) 8416–8418.
[41] M. Marrony, R. Barrera, S. Quenet, S. Ginocchio, L. Montelatici, A. Aslanides, Journal of Power Sources 182 (2008) 469–475.
[42] K.D. Kreuer, M. Schuster, B. Obliers, O. Diat, U. Traub, A. Fuchs, U. Klock, S.J. Paddison, J. Maier, Journal of Power Sources 178 (2008) 499–509.
[43] Q. Chen, K. Schmidt-Rohr, Macromolecules 37 (2004) 5995–6003.
[44] K.D. Kreuer, S.J. Paddison, E. Spohr, M. Schuster, Chemical Reviews 104 (2004) 4637–4678.
[45] L. Ghassemzadeh, K.D. Kreuer, J. Maier, K. Müller, in preparation.